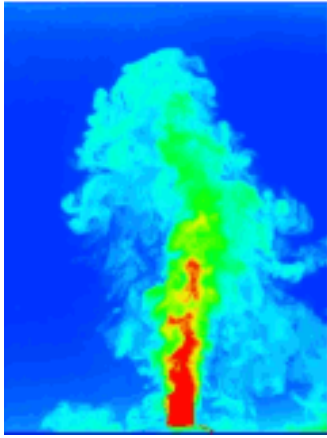


This article was downloaded by: [Tsinghua University]

On: 12 November 2014, At: 17:04

Publisher: Taylor & Francis

Informa Ltd Registered in England and Wales Registered Number: 1072954 Registered office: Mortimer House, 37-41 Mortimer Street, London W1T 3JH, UK



Journal of Turbulence

Publication details, including instructions for authors and subscription information:

<http://www.tandfonline.com/loi/tjot20>

Comparisons of different implementations of turbulence modelling in lattice Boltzmann method

Zhenhua Xia^a, Yipeng Shi^a, Yu Chen^b, Moran Wang^b & Shiyi Chen^a

^a State Key Laboratory for Turbulence and Complex Systems, CAPT and Department of Aeronautics and Astronautics, College of Engineering, Peking University, Beijing, China

^b Department of Engineering Mechanics, School of Aerospace, Tsinghua University, Beijing, China

Published online: 10 Oct 2014.

To cite this article: Zhenhua Xia, Yipeng Shi, Yu Chen, Moran Wang & Shiyi Chen (2015) Comparisons of different implementations of turbulence modelling in lattice Boltzmann method, *Journal of Turbulence*, 16:1, 67-80, DOI: [10.1080/14685248.2014.954709](https://doi.org/10.1080/14685248.2014.954709)

To link to this article: <http://dx.doi.org/10.1080/14685248.2014.954709>

PLEASE SCROLL DOWN FOR ARTICLE

Taylor & Francis makes every effort to ensure the accuracy of all the information (the "Content") contained in the publications on our platform. However, Taylor & Francis, our agents, and our licensors make no representations or warranties whatsoever as to the accuracy, completeness, or suitability for any purpose of the Content. Any opinions and views expressed in this publication are the opinions and views of the authors, and are not the views of or endorsed by Taylor & Francis. The accuracy of the Content should not be relied upon and should be independently verified with primary sources of information. Taylor and Francis shall not be liable for any losses, actions, claims, proceedings, demands, costs, expenses, damages, and other liabilities whatsoever or howsoever caused arising directly or indirectly in connection with, in relation to or arising out of the use of the Content.

This article may be used for research, teaching, and private study purposes. Any substantial or systematic reproduction, redistribution, reselling, loan, sub-licensing, systematic supply, or distribution in any form to anyone is expressly forbidden. Terms &

Conditions of access and use can be found at <http://www.tandfonline.com/page/terms-and-conditions>

Comparisons of different implementations of turbulence modelling in lattice Boltzmann method

Zhenhua Xia^{a*}, Yipeng Shi^a, Yu Chen^b, Moran Wang^b and Shiyi Chen^a

^aState Key Laboratory for Turbulence and Complex Systems, CAPT and Department of Aeronautics and Astronautics, College of Engineering, Peking University, Beijing, China; ^bDepartment of Engineering Mechanics, School of Aerospace, Tsinghua University, Beijing, China

(Received 1 April 2014; accepted 9 August 2014)

In this paper, we present an alternative approach for the turbulence modelling in the single-relaxation-time lattice Boltzmann method (LBM) framework by treating the turbulence term as an extra forcing term, in addition to the traditional approach of modifying the relaxation time. We compare these two different approaches and their mixture in large-eddy simulation (LES) of three-dimensional decaying isotropic homogenous turbulence using the Smagorinsky model and the mixed similarity model. When the LES was conducted using the Smagorinsky model, where the Boussinesq eddy-viscosity approximation is adopted, the results showed that these three different implementations are equivalent. However, when the mixed similarity model is adopted, which is beyond the Boussinesq eddy-viscosity approximation, our results showed that an equivalent eddy-viscosity will lead to errors, while the forcing approach is more straightforward and accurate. This provides an alternative and more general framework of simulation of turbulence with models in LBM, especially when the Boussinesq eddy-viscosity approximation is invalid.

Keywords: turbulence modelling; lattice Boltzmann method; Smagorinsky model; decaying isotropic homogenous turbulence

1. Introduction

The lattice Boltzmann method (LBM) [1,2], an alternative originated from the lattice gas automata [3] for solving the Navier–Stokes (NS) equations and modelling physics in fluids, has attracted considerable attention over the last two decades. The prevalence of this method is based upon its simple formulation, and the high level of suitability for computation on massive parallel computer clusters. It has been successfully applied in many fluid flow problems, including flows with simple or complex boundaries, two-phase flows, multi-component flows, turbulent flows and other complex flows [4–7] and proven to be an efficient and effective simulation tool.

The capability of the LBM for direct numerical simulation (DNS) of turbulent flows was investigated right after its birth through comparison with the pseudo-spectral simulations of decaying turbulence [1,8] and turbulent shear flows [9–11]. The inertial range scaling of $k^{-5/3}$ was reproduced and very good agreement was found for global quantities. Yu et al. [12] did a DNS of the three-dimensional decaying isotropic homogenous

*Corresponding author. Email: xiazh@pku.edu.cn

turbulence (DIHT) in inertial and rotating reference frames and their results clearly indicate that the LBM captures the important features of decaying turbulence, in both inertial and rotating reference frames. Recently, Peng et al. [13] did a comprehensive comparison between the LBM and pseudo-spectral methods for DNS of the three-dimensional DIHT. The instantaneous velocity and vorticity fields, and statistical quantities, including the total energy and the energy spectrum, the dissipation rate, the root-mean-squared pressure fluctuation and the pressure spectrum, and the skewness and flatness of the velocity derivative, were compared. They concluded that the LBM is a reliable and accurate method for the DNS of decaying turbulence. Moreover, Wang et al. [14] did a three-dimensional forced turbulence simulation using the multiple-relaxation-time (MRT) lattice Boltzmann approach [15] together with the Guo's forcing method [16], and careful comparisons with the pseudo-spectral results were conducted. Chikatamarla and Karlin [17] used the entropic LBM [18] to simulate the turbulent channel flow and flow past a circular cylinder at $Re = 3300$.

When LBM is used to simulate turbulence incorporated with modelling approaches, the Boussinesq eddy-viscosity approximation is always adopted. Hou et al. [19] used the Smagorinsky subgrid-scale (SGS) model to modify the relaxation time in the LBE by the effective relaxation time $\tau^* = 3(\nu_T + \nu_0) + 1/2$, where ν_0 and ν_T are the kinetic viscosity and turbulent eddy-viscosity, respectively. They applied this method to study the dynamics and the Reynolds number dependence of the flow structures in a two-dimensional driven cavity flow and concluded that the combination of the LBM and the SGS model offers a promising approach for turbulent flow simulations. Following this work, Yu and Girimaji [20], Yu et al. [21,22], Orphee et al. [23], Dong et al. [24,25] and Premnath et al. [26,27] conducted large-eddy simulations (LESs) of different turbulent flows using the LBM, and the results are encouraging. Chen et al. [28,29] insightfully analysed the analogy between the turbulent fluctuations and micro-scale thermal fluctuations, and showed that modelling turbulence in terms of LBE is very effective due to the remarkable similarity between the two. Almost all research works mentioned above were based on the assumption of the Boussinesq eddy-viscosity approximation. However, not all turbulence models could be approximated by the Boussinesq eddy-viscosity approximation, such as the stress-transport model in Reynolds-averaged Navier–Stokes (RANS) [30], and the mixed (similarity or non-linear) models [31], the approximate deconvolution method (ADM) [32] and the constrained SGS models [33] in LES. A more general way to incorporate turbulence models into the LBM is still missing.

In fact, Sagaut [34] proposed an extension of the ADM for the lattice-Boltzmann-based LES approach. Malaspina and Sagaut [35] proposed a consistent SGS model for the LBM-LES. In this study, we are going to propose a different approach to incorporate the turbulence models in LBM, which is to treat the turbulent terms as an extra forcing term as usually done in traditional NS solvers.

The remaining part of the present work is organised as follows. Section 2 will be devoted to the numerical methods and flow parameters, including a review of the LBM with external forcing term, a discussion of turbulence modelling and three different implementations of turbulence models in LBM, and a short description of the flow parameters. The simulation results, including the validation of basic LBM code, and comparisons of the three implementations of the Smagorinsky model and the mixed similarity model in LBM-LES, will be presented in Section 3. The conclusions and discussions will be given in Section 4.

2. Numerical methods and flow parameters

2.1. Lattice Boltzmann method with external forcing term

In the present study, the single-relaxation-time lattice Boltzmann equation (LBE) with external forcing term is used [1,2,16]:

$$f_i(\mathbf{x} + \mathbf{e}_i \delta_t, t + \delta_t) = f_i(\mathbf{x}, t) - \frac{1}{\tau} \left[f_i(\mathbf{x}, t) - f_i^{(eq)}(\mathbf{x}, t) \right] + \delta_t g_i(\mathbf{x}, t). \quad (1)$$

Here, $f_i(\mathbf{x}, t)$ is the distribution function (DF) for particles with velocity \mathbf{e}_i at position \mathbf{x} and time t , δ_t is the time increment, $g_i(\mathbf{x}, t)$ is the forcing term as a result of the body force density \mathbf{F} . $f_i^{(eq)}$ is the equilibrium distribution function (EDF) and τ is the non-dimensional relaxation time. In what follows, the D3Q19 model will be used. The discrete velocities and related weighting factors are

$$\mathbf{e}_i = \begin{cases} (0, 0, 0) & w_i = 1/3, \quad i = 0, \\ (\pm 1, 0, 0)c, (0, \pm 1, 0)c, (0, 0, \pm 1)c & w_i = 1/18, \quad i = 1 - 6, \\ (\pm 1, \pm 1, 0)c, (0, \pm 1, \pm 1)c, (\pm 1, 0, \pm 1)c & w_i = 1/36, \quad i = 7 - 18, \end{cases} \quad (2)$$

where, $c = \delta_x/\delta_t = 1$ in lattice units (i.e. $\delta_x = \delta_t$).

The EDF for incompressible flow is [36]

$$f_i^{(eq)} = w_i \left\{ \delta\rho + \rho_0 \left[\frac{3\mathbf{e}_i \cdot \mathbf{u}}{c^2} + \frac{9(\mathbf{e}_i \cdot \mathbf{u})^2}{2c^4} - \frac{3u^2}{2c^2} \right] \right\}. \quad (3)$$

Guo's forcing term g_i [16] is adopted here due to its comprehensive consideration on both the discrete lattice effect and the contributions of the body force to the momentum flux. It reads as

$$g_i = \left(1 - \frac{1}{2\tau} \right) \rho_0 w_i \left[\frac{3(\mathbf{e}_i - \mathbf{u})}{c^2} + \frac{9(\mathbf{e}_i \cdot \mathbf{u})}{c^4} \mathbf{e}_i \right] \cdot \mathbf{F}, \quad (4)$$

where $\delta\rho$ is the density fluctuation, ρ_0 is the constant mean density in the system which is usually set to 1. The total density is $\rho = \rho_0 + \delta\rho$. The sound speed of the model is $c_s = c/\sqrt{3}$. The macro quantities $\delta\rho$ and \mathbf{u} are related to the DF as

$$\delta\rho = \sum_i f_i, \quad \rho_0 \mathbf{u} = \sum_i \mathbf{e}_i f_i + \frac{\delta_t}{2} \rho_0 \mathbf{F}. \quad (5)$$

Through the Chapman–Enskog analysis, the above LBE leads to the following macroscopic equations:

$$\partial_t \delta\rho + \rho_0 \nabla \cdot \mathbf{u} = 0, \quad (6)$$

$$\partial_t \mathbf{u} + \nabla \cdot (\mathbf{u}\mathbf{u}) = -\frac{1}{\rho_0} \nabla p + \nabla \cdot [\nu(\nabla \mathbf{u} + (\nabla \mathbf{u})^T)] + \mathbf{F}, \quad (7)$$

with $p = c_s^2 \delta\rho$ and the kinetic viscosity $\nu = 1/3(\tau - 1/2)c^2 \delta_t$. Note that the $\delta\rho$ in the above equations could be replaced by ρ since ρ_0 is constant.

The strain rate tensor $S_{ij} = 1/2(\partial u_i/\partial x_j + \partial u_j/\partial x_i)$ can always be calculated using the macroscopic quantities directly by the finite-difference scheme. However, in LBM, S_{ij} can alternatively be obtained through the DFs as

$$S_{ij} = -\frac{3}{2\rho_0 c^2 \tau \delta_t} Q_{ij} - \frac{3}{4c^2 \tau} (u_i F_j + u_j F_i), \quad Q_{ij} = \sum_k e_{ki} e_{kj} [f_k - f_k^{(\text{eq})}]. \quad (8)$$

2.2. Turbulence modelling

In turbulent flow, the Reynolds number is usually very high. In this situation, DNS is very expensive, therefore turbulence modelling approaches are very plausible, among which are the most used RANS equations and LES. When turbulence modelling is adopted in LBM, Equation (1) will be modified as

$$\hat{f}_i(\mathbf{x} + \mathbf{e}_i \delta_t, t + \delta_t) = \hat{f}_i(\mathbf{x}, t) - \frac{1}{\tau_*} [\hat{f}_i(\mathbf{x}, t) - \hat{f}_i^{(\text{eq})}(\mathbf{x}, t)] + \delta_t \hat{g}_i^*(\mathbf{x}, t), \quad (9)$$

with τ_* and \hat{g}_i^* as the modified relaxation time and forcing term, respectively.

The corresponding modelled macroscopic equations are

$$\partial_t \widehat{\rho} + \rho_0 \nabla \cdot \hat{\mathbf{u}} = 0, \quad (10)$$

$$\partial_t \hat{\mathbf{u}} + \nabla \cdot (\hat{\mathbf{u}} \hat{\mathbf{u}}) = -\frac{1}{\rho_0} \nabla \hat{p} + \nabla \cdot [\nu_* (\nabla \hat{\mathbf{u}} + (\nabla \hat{\mathbf{u}})^T)] + \hat{\mathbf{F}}^*, \quad (11)$$

where the ‘hat’ denotes the averaging process for RANS or filtering process for LES, and ν_* and $\hat{\mathbf{F}}^*$ are the corresponding viscosity and the external body force.

Meanwhile, when the ‘hat’ operation is applied to Equations (6) and (7), we have

$$\partial_t \widehat{\rho} + \rho_0 \nabla \cdot \hat{\mathbf{u}} = 0, \quad (12)$$

$$\partial_t \hat{\mathbf{u}} + \nabla \cdot (\hat{\mathbf{u}} \hat{\mathbf{u}}) = -\frac{1}{\rho_0} \nabla \hat{p} + \nabla \cdot [\nu (\nabla \hat{\mathbf{u}} + (\nabla \hat{\mathbf{u}})^T)] + \hat{\mathbf{F}} - \nabla \cdot \mathbf{T}, \quad (13)$$

where $\mathbf{T} = \widehat{\mathbf{u}} \hat{\mathbf{u}} - \hat{\mathbf{u}} \hat{\mathbf{u}}$ is the resulting extra term, i.e. Reynolds stresses for RANS or SGS stresses for LES. Comparison between the above Equations (10)–(11) and (12)–(13) will provide the basic ideas of implementations of turbulence modelling in the LBM framework.

If the Boussinesq eddy-viscosity approximation is adopted in Equation (13), then T_{ij} could be modelled by $-2\nu_t \hat{S}_{ij}$, with ν_t the eddy-viscosity for RANS or LES. Then, in LBM, two instinctive different implementations can be used to take this extra term into account. One is to absorb the eddy-viscosity into the physical viscosity, resulting in the total effective viscosity $\nu_* = \nu + \nu_t$ in Equation (11), while the forcing term keeps the same; and the other is to maintain the physical viscosity, while the extra term $-\nabla \cdot \mathbf{T}$ is added to the external forcing term in Equation (11).

In the former one (referred as approach A1), a total effective relaxation time τ_* can be related to the effective viscosity ν_* as

$$\tau_* = \tau + \tau_t = \frac{1}{2} + \frac{3\nu_*}{c^2\delta_t}, \quad (14)$$

where, $\tau_t = 3\nu_t/(c^2\delta_t)$ is the relaxation time corresponding to the turbulent eddy-viscosity ν_t . This implementation is quite straightforward and one only needs to change the relaxation time in the LBE-DNS code to run the LBE-LES simulation.

In the latter one (referred as approach A2), the relaxation time keeps unchanged, i.e. $\tau_* = \tau = 1/2 + 3\nu/(c^2\delta_t)$, but the forcing term is modified as

$$\hat{g}_i^* = \left(1 - \frac{1}{2\tau_*}\right) \rho_0 w_i \left[\frac{3(\mathbf{e}_i - \mathbf{u})}{c^2} + \frac{9(\mathbf{e}_i \cdot \mathbf{u})}{c^4} \mathbf{e}_i \right] \cdot \hat{\mathbf{F}}^*, \quad (15)$$

with $\hat{\mathbf{F}}^* = \hat{\mathbf{F}} + \nabla \cdot (2\nu_t \mathbf{S})$. In this implementation, one has to calculate the divergence of turbulent stresses, which is a little more time consuming.

Nevertheless, the turbulence term can always be divided into two parts, $\mathbf{T} = \mathbf{T}_1 + \mathbf{T}_2$, with \mathbf{T}_1 being used in the approach A1 and \mathbf{T}_2 being used in the approach A2 (this will be referred as the mixed approach or approach A3). In the appendix of a paper by Premnath et al. [27], they mentioned about this mixed approach of incorporation of the dynamic mixed model and dynamic two-parameter SGS model in MRT-LBM. However, no simulation results or comparison results were shown.

In fact, not all turbulence models could be approximated by the Boussinesq eddy-viscosity approximation, such as the stress-transport model in RANS [30], and the mixed (similarity or non-linear) models [31,37] and the constrained SGS models [33] in LES. In this case, one may obtain an approximated equivalent eddy-viscosity by the least-square method and adopt the approach A1. However, this could inevitably lead to some errors. A more accurate way is to directly employ the approach A2 or the mixed approach A3.

In the following part, we will take the Smagorinsky SGS model [31,38] and the mixed similarity model [31,37,39–41] as examples for the turbulence term. In the Smagorinsky model, the SGS eddy-viscosity ν_t is calculated from the filtered strain rate tensor \tilde{S}_{ij} and a filter width Δ :

$$\nu_t = (C_s \Delta)^2 |S|. \quad (16)$$

Here, C_s is the model coefficient, and $|S| = \sqrt{2\tilde{S}_{ij}\tilde{S}_{ij}}$ is the characteristic filtered rate of strain with \tilde{S}_{ij} being calculated using Equation (8) or using other traditional finite-difference scheme. In the mixed similarity model, the SGS stress is evaluated as

$$T_{ij} = (\overline{\tilde{u}_i \tilde{u}_j} - \tilde{u}_i \tilde{u}_j) - 2(C_s \Delta)^2 |S| \tilde{S}_{ij}. \quad (17)$$

Here, ‘bar’ denotes a filtering operation at a test-filter scale $\bar{\Delta} = 2\Delta$. Usually, the model coefficient C_s is computed through a dynamic procedure in mixed similarity model [37,39,41]. However, for simplicity, we chose to use a constant value $C_s = 0.1$ as evaluated from a-priori experiment test [40].

If approach A1 is used in Smagorinsky model, then the turbulent relaxation time τ_t could be calculated explicitly by its definition, where $|S|$ is calculated using τ_* at the previous

Table 1. Flow parameters for DIHT.

Solver	Model	N^3	ν	δ_t	τ	V_{scale}
PS	DNS	128^3	0.01	0.001	–	–
LBM	DNS	128^3	2.037×10^{-4}	$2\pi/128$	0.5125	2.037×10^{-2}
LBM	LES-SM	64^3	1.019×10^{-4}	$2\pi/64$	0.5031	1.019×10^{-2}
LBM	LES-MS	64^3	1.019×10^{-4}	$2\pi/64$	0.5031	1.019×10^{-2}

Note: SM, Smagorinsky model; MS, mixed similarity model.

time step. However, one can also calculate it implicitly at current time step as [19,21,42]

$$\tau_t = \frac{1}{2} \left(\sqrt{\tau^2 + \frac{2(C_s \Delta)^2}{\rho_0 c_s^4 \delta_t^2} \sqrt{2\hat{Q}_{ij}\hat{Q}_{ij}} - \tau} \right). \quad (18)$$

2.3. Flow parameters

In this study, the three-dimensional DIHT is simulated by LBM using both DNS and LES approaches. The simulations were conducted on a cubic box with size $L^3 = (2\pi)^3$ and grid resolution N^3 . The physical kinetic viscosity $\nu_s = 0.01$ and related physical time step is $dt_s = 0.001$. In LBM, $\delta_x = \delta_t = 2\pi/N$. The flow parameters are listed in Table 1.

The initial velocity field was obtained from a separated DNS of stationary isotropic homogenous turbulence using the pseudo-spectral method with the same flow parameters and grid resolution. The forcing was implemented at the large scales by fixing the kinetic energy at first two wave numbers. The initial Taylor micro-scale Reynolds number was kept $Re_\lambda \approx 47.8$. Then, the velocity field was rescaled to the lattice frame by a velocity scale V_{scale} to make sure that $Ma_{\text{max}} = \|\mathbf{u}\|_{\text{max}}/c_s \leq 0.15$. The initial density fluctuation $\delta\rho$ and DFs f_i can then be obtained by an iteration procedure [12,13,21]. As discussed by Yu et al. [21], this iteration procedure can minimise the errors due to the initialisation of LBE. The viscosity in lattice units is related to the physical viscosity by $\nu = \nu_s \times V_{\text{scale}}$.

3. Results

In this section, we present the results of our numerical simulations. First, we are going to validate our basic LBM code by comparing the DNS results with those from pseudo-spectral method under the same conditions. Then simulations with three different LBM-LES implementations of two different SGS models were carried out and put into comparison.

3.1. Validation of the basic LBM code

In this subsection, the DNSs of the DIHT were carried out using LBM (LB-DNS) and pseudo-spectral (PS-DNS) methods with $N = 128$.

Figure 1 shows the energy spectra from both LB-DNS and PS-DNS at different time points. Since the de-aliasing is accomplished by nullifying $\hat{u}_i(k_i, t)$ for $k = \sqrt{k_1^2 + k_2^2 + k_3^2} > N/3$ in the pseudo-spectral method, its actual wave numbers are $k \leq N/3$. However in LB-DNS, its actual wave numbers can be $k \leq N/2$. It is clearly seen

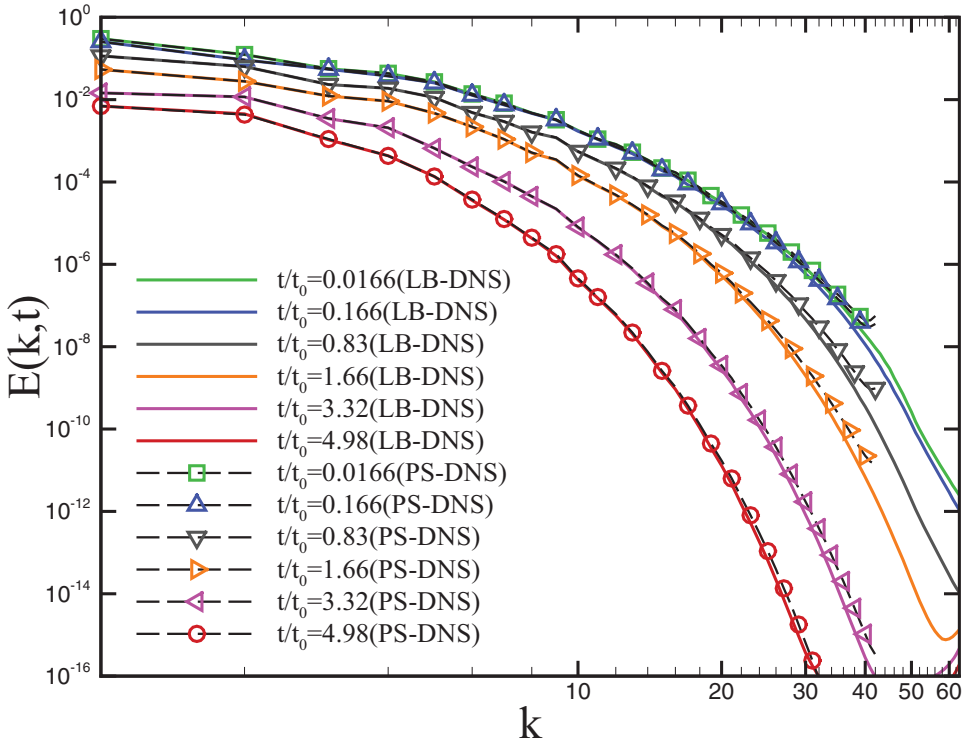


Figure 1. The energy spectra $E(k, t)$ from different numerical methods at different time points. Solid lines are from DNS with LBM (denoted as LB-DNS) and dashed lines with symbols are from pseudo-spectral method (denoted as PS-DNS).

from this figure that the spectra from the two different methods match very well with each other at lower wave numbers, where most of the kinetic energy is preserved, and the deviations emerge first at wave number near $k \sim N/3$ and then move to smaller wave numbers as time evolves. These slight differences on spectra at high wave numbers will not cause significant deviations on the integral quantities, such as the normalised kinetic energy $k(t)/k_0$ and the normalised dissipation rate $\epsilon(t)/\epsilon_0$, as shown in Figure 2. From these comparisons, we can assure that our basic LBM code is correct and reliable.

3.2. Comparisons of different implementations of the Smagorinsky model in LBM-LES

In this subsection, we will compare the LES results from three different implementations of the Smagorinsky SGS model in LBM simulations with $C_s = 0.17$. In the mixed approach, the two parts were half and half. The results from approaches A1, A2 and A3 are denoted as SM-A1, SM-A2 and SM-A3, respectively.

In Figure 3, we are showing the energy spectra $E(k, t)$ from the three above-discussed implementations of the Smagorinsky SGS model at four different time, i.e. $t/t_0 = 0.0166, 0.166, 0.83$ and 1.66 . Clearly, the differences on the spectra are negligible and those spectra from the SM-A3 lie between those from SM-A1 and SM-A2. These negligible deviations

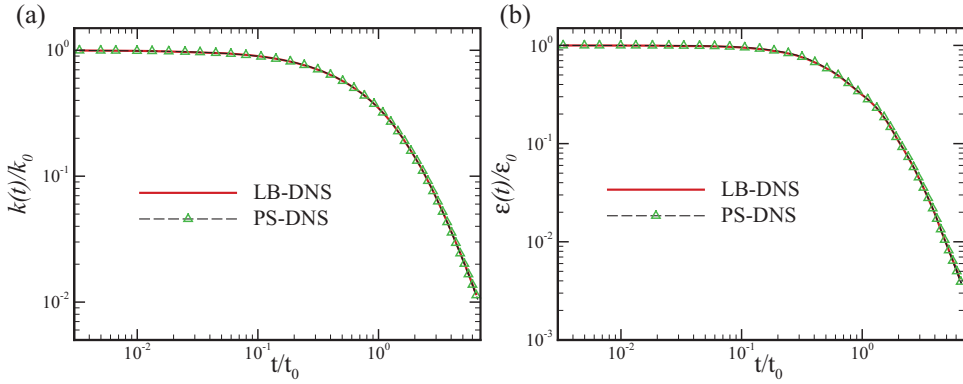


Figure 2. Time evolution of the normalised kinetic energy $k(t)/k_0$ (a) and the normalised dissipation rate $\epsilon(t)/\epsilon_0$ (b) from different numerical methods: LB-DNS and PS-DNS.

in spectra result in almost the same statistical quantities, such as the normalised kinetic energy $k(t)/k_0$ shown in Figure 4 and the flow fields shown in Figure 5.

Figure 5 shows the contours of u from the three different implementations of the Smagorinsky SGS model on the plane $z = \pi$ at $t/t_0 = 0.166$ (panel (a)) and $t/t_0 = 1.66$ (panel (b)). Clearly, the flow fields are still the same even after it evolves a time period of $1.66t_0$. From this comparison, we may conclude that the three different implementations of turbulence models under the Boussinesq eddy-viscosity approximation are equivalent.

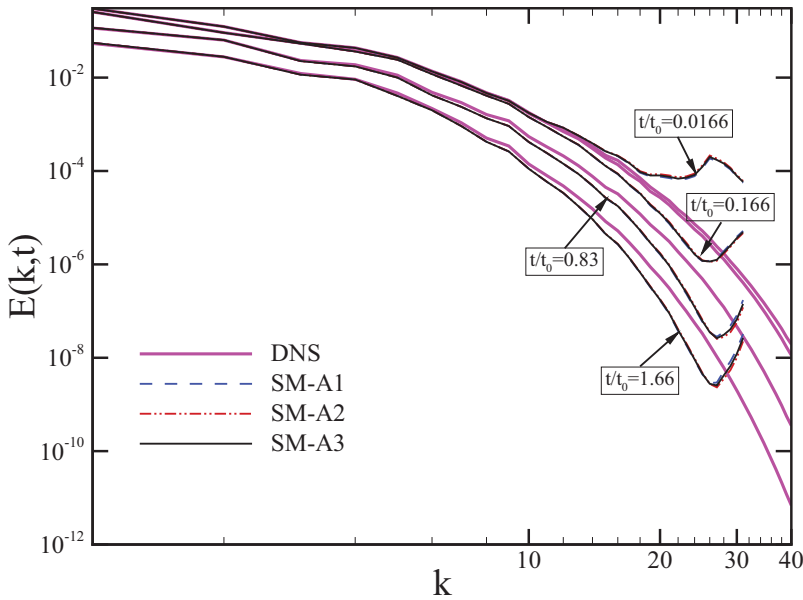


Figure 3. The energy spectra $E(k, t)$ from three different implementations of the Smagorinsky SGS model at different time points. Dashed lines are from SM-A1, dash-double-dotted lines are from SM-A2 and solid lines are from SM-A3. The thick solid lines from LB-DNS are used as references.

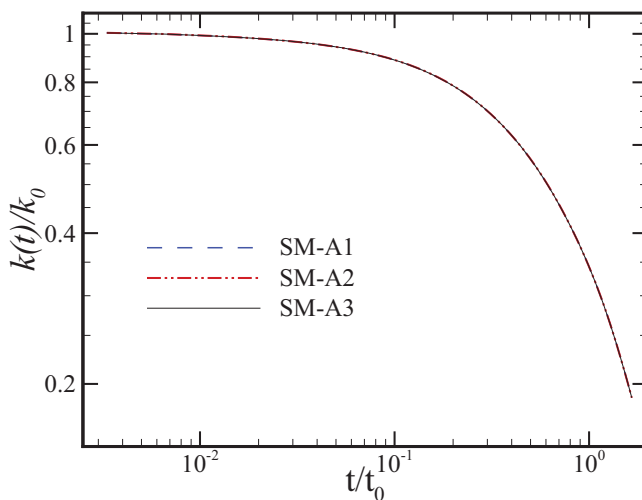


Figure 4. Time evolution of the normalised kinetic energy $k(t)/k_0$ from three different implementations of the SGS model.

3.3. Comparisons of different implementations of the mixed similarity model in LBM-LES

In this subsection, we will compare the LES results from three different implementations of the mixed similarity SGS model in LBM simulations with $C_s = 0.1$. In approach A1, we approximated the SGS stress by introducing an equivalent eddy-viscosity as

$$\hat{\nu}_t = \frac{-T_{ij}\tilde{S}_{ij}}{2\tilde{S}_{ij}\tilde{S}_{ij}} = \frac{-(\tilde{u}_i\tilde{u}_j - \tilde{u}_i\tilde{u}_j)\tilde{S}_{ij}}{2\tilde{S}_{ij}\tilde{S}_{ij}} + (C_s\Delta)^2|S|. \quad (19)$$

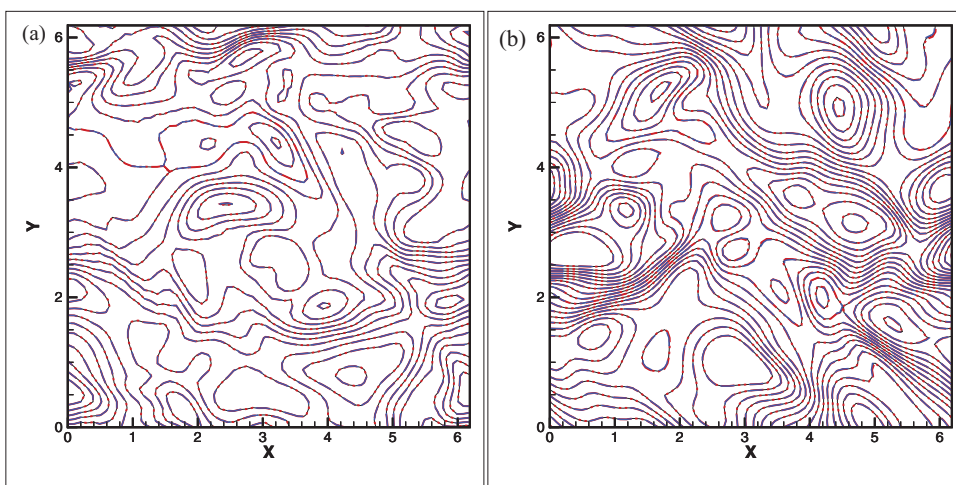


Figure 5. Contours of u from three different implementations of the Smagorinsky SGS model on the plane $z = \pi$ at different time points: (a) $t/t_0 = 0.166$; (b) $t/t_0 = 1.66$. Dashed lines are from LES-A1; dash-double-dotted lines are from LES-A2 and solid lines are from LES-A3.

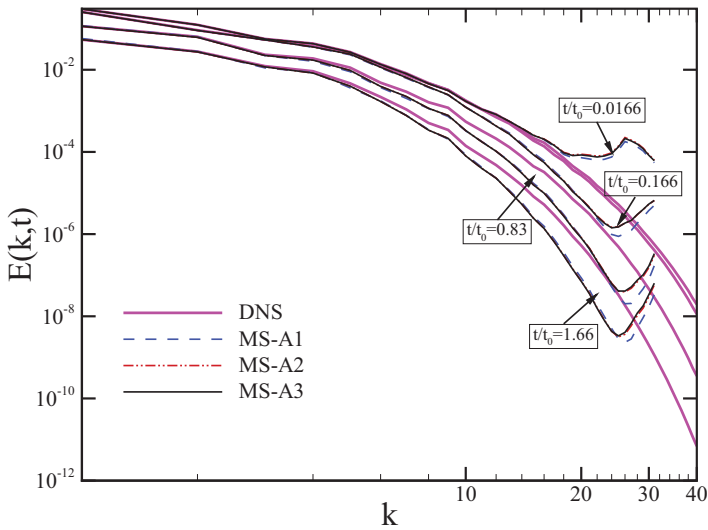


Figure 6. The energy spectra $E(k, t)$ from three different implementations of the mixed similarity SGS model at different time points. Dashed lines are from MS-A1, dash-double-dotted lines are from MS-A2 and solid lines are from MS-A3. The thick solid lines from LB-DNS are used as references.

In the mixed approach A3, the dissipation part (Smagorinsky part) was implemented using approach A1 while the similarity part was planted using approach A2. Clearly, when the mixed similarity SGS model is used, approach A1 is only an approximation, which inevitably leads to errors; while approaches A2 and A3 are accurate. In the following, the results from approaches A1, A2 and A3 will be denoted as MS-A1, MS-A2 and MS-A3, respectively.

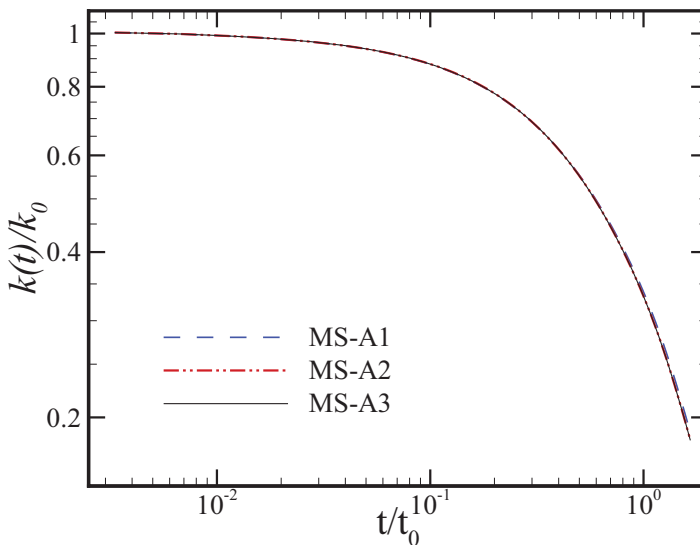


Figure 7. Time evolution of the normalised kinetic energy $k(t)/k_0$ from three different implementations of the mixed similarity SGS model.

In Figure 6, we are showing the energy spectra $E(k, t)$ from the three above-discussed implementations of the mixed similarity SGS model at four different time points, i.e. $t/t_0 = 0.0166, 0.166, 0.83$ and 1.66 . It can be clearly seen that the spectra from MS-A2 and MS-A3 are almost the same at all wave numbers, while those from MS-A1 deviate from those from MS-A2 and MS-A3 at high wave numbers ($k \gtrsim 21$). However, these differences at high wave numbers do not result in significant deviations on the statistical quantities, such as the normalised kinetic energy $k(t)/k_0$ shown in Figure 7, but cause significant disparities in single flow fields as shown in Figure 8.

Figure 8 shows the contours of u from the three different implementations of the Smagorinsky SGS model on the plane $z = \pi$ at $t/t_0 = 0.083$ (panel (a)), $t/t_0 = 0.166$ (panel (b)), $t/t_0 = 0.83$ (panel (c)) and $t/t_0 = 1.66$ (panel (d)). Obviously, the flow fields from these three different implementations are almost the same at early stage ($t/t_0 = 0.083$, panel (a)). However, as time evolves, the flow fields from MS-A2 and MS-A3 still keep the same while

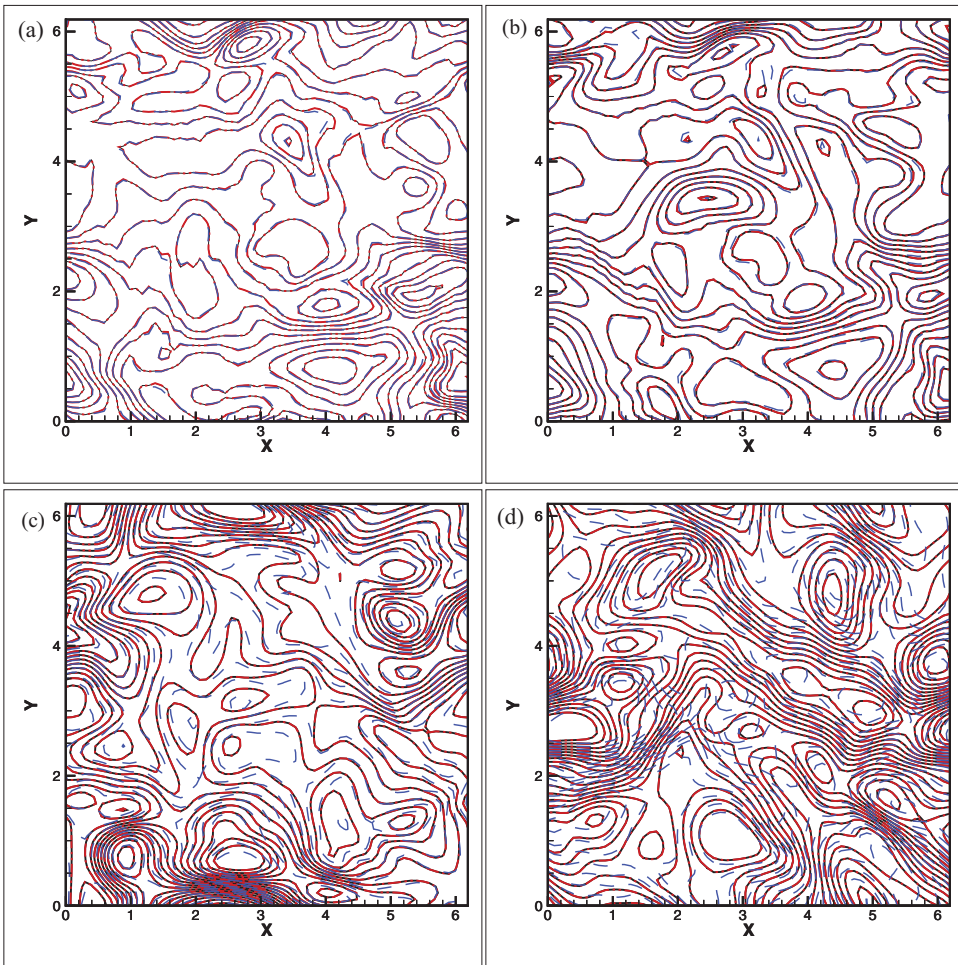


Figure 8. Contours of u from three different implementations of the mixed similarity SGS model on the plane $z = \pi$ at different time points: (a) $t/t_0 = 0.083$; (b) $t/t_0 = 0.166$; (c) $t/t_0 = 0.83$; (d) $t/t_0 = 1.66$. Dashed lines are from MS-A1, dash-double-dotted lines are from MS-A2 and solid lines are from MS-A3.

the disparities between those from MS-A1 and MS-A2 emerge and become more and more apparent. These disparities are believed to come from the approximation of the similarity part in the mixed similarity model by an equivalent eddy-viscosity $\hat{\nu}_t$, as discussed above.

From the above comparison, we may conclude that the three different implementations of turbulence models beyond the Boussinesq eddy-viscosity approximation are not equivalent. The idea of introducing an equivalent eddy-viscosity will inevitably lead to some errors. This might indicate that the implementation of turbulence models in the LBM through forcing term is a more general approach.

4. Conclusions and discussions

In the simulation of turbulence with modelling approach in the LBM framework, the most popular way is to modify the relaxation time based on the Boussinesq eddy-viscosity approximation. However, not all turbulence models can be approximated by the Boussinesq eddy-viscosity assumption, which raises some difficulties in this traditional approach. An alternative and more general way¹ is to treat the turbulence term as an extra forcing term.

This study first reviewed the single-relaxation-time LBE with extra forcing terms and the relative macro–meso relations. The Chapman–Enskog expansion shows that the strain rate tensor is related to the DFs as well as the extra forces.

When a turbulence modelling approach is incorporated into the LBM, three different implementations can be adopted, i.e. the widely used modification of the relaxation time (A1), the extra forcing approach (A2) and the mixed approach (A3). We compare these three different approaches in LES of three-dimensional DIHT using the Smagorinsky model and the mixed similarity model. When the LES was conducted using the Smagorinsky model, where the Boussinesq eddy-viscosity approximation is adopted, the results showed that these three different implementations are equivalent. However, when the mixed similarity model is adopted, which is beyond the Boussinesq eddy-viscosity approximation, our results showed that an equivalent eddy-viscosity will lead to errors, while the forcing approach is more straightforward and accurate. This provides an alternative and more general framework of simulation of turbulence with models in LBM, especially when the Boussinesq eddy-viscosity approximation is invalid.

In the future, comparisons with different turbulent models in forced isotropic turbulence can be conducted, where more quantities, such as energy flux, the high-order moments of longitudinal velocity increment or the extended self-similarity [44,45] behaviour, could be compared. Also, we will compare these three different implementations of turbulent models in more complex flow problems. Furthermore, we hope that these different approaches of incorporating the turbulence models into LBM may inspire developing of new turbulence methods in gas-kinetic schemes.

Acknowledgements

We appreciate Lianping Wang and Zuoli Xiao for many useful discussions. Numerical simulations were finished at Dawn clusters in Peking University.

Funding

We acknowledge the financial support provided by National Natural Science Foundation of China [grant number 91130001], [grant number 11221061], [grant number 11302006]. Author Z. Xia wants to thank the support from National Science Foundation for Postdoctoral Scientists of China [grant number 2012M520109].

Note

1. As pointed out by one of the referees that the word ‘general’ here is somewhat misleading. We would like to emphasise here that the word ‘general’ focuses on the capability to treat different types, within or beyond the Boussinesq approximation, of turbulence models. When LBM is used to simulate turbulence incorporated with modelling approaches, different perspectives exist. If a turbulence model (SGS or RANS) was derived through the Boltzmann equation based on the kinetic theory, then the notion of effective relaxation time is way more general [28,43]. From this perspective, a well-defined characteristic relaxation time scale could describe self-consistent dynamics of turbulent fluctuations better, and usually the notion of eddy-viscosity was adopted, as reviewed in this paper, to estimate the effective relaxation time in applications. However, if we viewed LBM as a tool to solve the Navier–Stokes (NS) equations, then we might use the extended LBE (Equation (9)) to solve flow problems incorporated with turbulence models (RANS or LES models) instead. From this perspective, LBM is just a special solver, as the finite-volume method, to NS equations, and we could adopt any type of turbulence models, within or beyond eddy-viscosity assumption, as claimed in this work. If we further took the notion of eddy-viscosity, we could simply use the effective relaxation time to account for the turbulence models. At this point, these two different perspectives reach the same formulas.

References

- [1] H. Chen, S. Chen, and H. Matthaeus, *Recovery of the Navier-Stokes equation using a lattice Boltzmann method*, Phys. Rev. A 45 (1992), pp. R5339–R5342.
- [2] Y. Qian, D. d’Humières, and P. Lallemand, *Lattice BGK models for Navier-Stokes equations*, Europhys. Lett. 17 (1992), pp. 479–484.
- [3] F. Higuera, S. Succi, and R. Benzi, *Lattice gas dynamics with enhanced collisions*, Europhys. Lett. 9 (1989), pp. 345–349.
- [4] R. Benzi, S. Succi, and M. Vergassola, *The lattice Boltzmann equation: Theory and applications*, Phys. Rep. 222 (1992), pp. 145–197.
- [5] S. Chen and G. Doolen, *Lattice Boltzmann method for fluid flows*, Annu. Rev. Fluid Mech. 30 (1998), pp. 329–364.
- [6] D. Yu, R. Mei, L. Luo, and W. Shyy, *Various flow computations with the method of lattice Boltzmann equation*, Prog. Aerosp. Sci. 39 (2003), pp. 329–367.
- [7] C. Aidun and J. Clausen, *Lattice Boltzmann method for complex flows*, Annu. Rev. Fluid Mech. 42 (2010), pp. 439–472.
- [8] D. Martinez, W. Matthaeus, S. Chen, and D. Montgomery, *Comparison of spectral method and lattice Boltzmann simulations of two-dimensional hydrodynamics*, Phys. Fluids 6 (1994), pp. 1285–1298.
- [9] R. Benzi and S. Succi, *Two-dimensional turbulence with the lattice Boltzmann equation*, J. Phys. A 23 (1990), pp. L1–5.
- [10] Y. Qian, S. Succi, and S. Orszag, *Recent advances in lattice Boltzmann computing*, Annu. Rev. Comput. Phys. 3 (1995), pp. 195–242.
- [11] J. Eggels, *Direct and large-eddy simulation of turbulent fluid flow using the lattice-Boltzmann scheme*, Int. J. Heat Fluid Flow 17 (1996), pp. 307–323.
- [12] H. Yu, S. Girimaji, and L. Luo, *Lattice Boltzmann simulations of decaying homogeneous isotropic turbulence*, Phys. Rev. E 71 (2005), 016708.
- [13] Y. Peng, W. Liao, L. Luo, and L. Wang, *Comparison of the lattice Boltzmann and pseudo-spectral methods for decaying turbulence: Low-order statistics*, Comput. Fluids 39 (2010), pp. 568–591.
- [14] L. Wang, O. Ayala, H. Gao, C. Andersen, and K. Mathews, *Study of forced turbulence and its modulation by finite-size solid particles using the lattice Boltzmann approach*, Comput. Math. Appl. 67 (2014), pp. 363–380.
- [15] D. d’Humières, I. Ginzburg, M. Krafczyk, P. Lallemand, and L.S. Luo, *Multiple-relaxation-time lattice Boltzmann models in three-dimensions*, Philos. Trans. R. Soc. Lond. A Math. Phys. Eng. Sci. 360 (2002), pp. 437–451.
- [16] Z. Guo, C. Zheng, and B. Shi, *Discrete lattice effects on the forcing term in the lattice Boltzmann method*, Phys. Rev. E 65 (2002), 046308.

- [17] S. Chikatamarla and I. Karlin, *Entropic lattice Boltzmann method for turbulent flow simulations: Boundary conditions*, Phys. A 392 (2013), pp. 1925–1930.
- [18] S. Chikatamarla, S. Ansumali, and I. Karlin, *Entropic lattice Boltzmann models for hydrodynamics in three dimensions*, Phys. Rev. Lett. 97 (2006), 010201.
- [19] S. Hou, J. Sterling, S. Chen, and G. Doolen, *A lattice Boltzmann subgrid-scale model for high Reynolds number flows*, Fields Inst. Commun. 6 (1996), pp. 151–166.
- [20] H. Yu and S. Girimaji, *Near-field turbulent simulations of rectangular jets using lattice Boltzmann method*, Phys. Fluids 17 (2005), 125106.
- [21] H. Yu, S. Girimaji, and L. Luo, *DNS and LES of decaying isotropic turbulence with and without frame rotation using lattice Boltzmann method*, J. Comput. Phys. 209 (2005), pp. 599–616.
- [22] H. Yu, L. Luo, and S. Girimaji, *LES of turbulent square jet flow using an MRT lattice Boltzmann model*, Comput. Fluids 35 (2006), pp. 957–965.
- [23] J. Orphee, A. Gungor, M. Sanchez-Rocha, and S. Menon, *Direct and large-eddy simulation of decaying and forced isotropic turbulence using lattice Boltzmann method*, 36th AIAA Fluid Dynamics Conference and Exhibit, AIAA-2006-3904, San Francisco, CA, 2006.
- [24] Y. Dong and P. Sagaut, *A study of time correlations in lattice Boltzmann-based large-eddy simulation of isotropic turbulence*, Phys. Fluids 20 (2008), 035105.
- [25] Y. Dong, P. Sagaut, and S. Marie, *Inertial consistent subgrid model for large-eddy simulation based on the lattice Boltzmann method*, Phys. Fluids 20 (2008), 035104.
- [26] K. Premnath, M. Pattison, and S. Banerjee, *Generalized lattice Boltzmann equation with forcing term for computation of wall-bounded turbulent flows*, Phys. Rev. E 79 (2009), 026703.
- [27] K. Premnath, M. Pattison, and S. Banerjee, *Dynamic subgrid scale modeling of turbulent flows using lattice-Boltzmann method*, Phys. A 388 (2009), pp. 2640–2658.
- [28] H. Chen, S. Kandasamy, S. Orszag, R. Shock, S. Succi, and V. Yakhot, *Extended Boltzmann kinetic equation for turbulent flows*, Science 301 (2003), pp. 633–636.
- [29] H. Chen, S. Orszag, I. Staroselsky, and S. Succi, *Expanded analogy between Boltzmann kinetic theory of fluids and turbulence*, J. Fluid Mech. 519 (2004), pp. 301–314.
- [30] D. Wilcox, *Turbulence Modeling for CFD*, DCW Industries, La Cañada, CA, 2006.
- [31] S. Pope, *Turbulent Flows*, Cambridge University Press, Cambridge, UK, 2000.
- [32] S. Stolz and N. Adams, *An approximate deconvolution procedure for large-eddy simulation*, Phys. Fluids 11 (1999), pp. 1699–1701.
- [33] S. Chen, Z. Xia, S. Pei, J. Wang, Y. Yang, Z. Xiao, and Y. Shi, *Reynolds-stress-constrained large-eddy simulation of wall-bounded turbulent flows*, J. Fluid Mech. 703 (2012), pp. 1–28.
- [34] P. Sagaut, *Toward advanced subgrid models for lattice-Boltzmann-based large-eddy simulation: Theoretical formulations*, Comput. Math. Appl. 59 (2010), pp. 2194–2499.
- [35] O. Malaspinas and P. Sagaut, *Consistent subgrid scale modelling for lattice Boltzmann methods*, J. Fluid Mech. 700 (2012), pp. 514–542.
- [36] X. He and L. Luo, *Lattice Boltzmann model for the incompressible Navier–Stokes equation*, J. Stat. Phys. 88 (1997), pp. 927–944.
- [37] R. Anderson and C. Meneveau, *Effects of the similarity model in finite-difference LES of isotropic turbulence using a Lagrangian dynamic mixed model*, Flow Turbul. Combust. 62 (1999), pp. 201–225.
- [38] J. Smagorinsky, *General circulation experiments with the primitive equations: I. The basic equation*, Monthly Weather Rev. 91 (1963), pp. 99–164.
- [39] Y. Zang, R. Street, and J. Koseff, *A dynamic mixed subgrid-scale model and its application to turbulent recirculating flows*, Phys. Fluids A 5 (1993), pp. 3186–3196.
- [40] S. Liu, C. Meneveau, and J. Katz, *Experimental study of similarity subgrid-scale models of turbulence in the far-field of a jet*, Appl. Sci. Res. 54 (1995), pp. 177–190.
- [41] B. Vreman, B. Geurts, and H. Kuerten, *Large-eddy simulation of the turbulent mixing layer*, J. Fluid Mech. 339 (1997), pp. 357–390.
- [42] J. Li and Z. Wang, *An alternative scheme to calculate the strain rate tensor for the LES applications in the LBM*, Math. Prob. Eng. 2010 (2010), 724578.
- [43] S. Ansumali, I. Karlin, and S. Succi, *Kinetic theory of turbulence modeling: Smallness parameter, scaling and microscopic derivation of Smagorinsky model*, Phys. A 338 (2004), pp. 379–394.
- [44] R. Benzi, S. Ciliberto, R. Tripiccion, C. Baudet, F. Massaioli, and S. Succi, *Extended self-similarity in turbulent flows*, Phys. Rev. E 48 (1993), pp. R29–R32.
- [45] M. Briscolini, P. Santangelo, S. Succi, and R. Benzi, *Extended self-similarity in the numerical simulation of three-dimensional homogeneous flows*, Phys. Rev. E 50 (1994), pp. R1745–R1747.